

# 1 Integrative Proximal-Ubiquitomics Profiling for Deubiquitinase and 2 E3 Ligase Substrate Discovery Applied to USP30

3

4 Andreas Damianou<sup>1,2\*†</sup>, Hannah B.L. Jones<sup>1\*†</sup>, Athina Grigoriou<sup>1</sup>, Iolanda Vendrell<sup>1,2</sup>, Simon  
5 Davis<sup>1,2</sup>, Benedikt M. Kessler<sup>1,2\*</sup>

6

7 <sup>1</sup>Target Discovery Institute, Centre for Medicines Discovery, Nuffield Department of  
8 Medicine, University of Oxford, Roosevelt Drive, Oxford OX3 7FZ, UK

9 <sup>2</sup>Chinese Academy for Medical Sciences Oxford Institute, Nuffield Department of Medicine,  
10 University of Oxford, Roosevelt Drive, Oxford OX3 7FZ, UK

11

12 <sup>†</sup> These authors contributed equally

13

14 \*Corresponding author(s): HBLJ, AD, BMK

15 H.B.L.J. email: hannah.jones@ndm.ox.ac.uk

16 A.D. email: andreas.damianou@ndm.ox.ac.uk

17 B.M.K. email: benedikt.kessler@ndm.ox.ac.uk

18

19

20

21 Running Title: Proximal-ubiquitomics facilitates USP30 substrate discovery

22

23

24

25

26 Key Words: APEX2, proximity labelling, deubiquitinase, ubiquitin specific protease 30, USP30,

27 LETM1, mass spectrometry, proteomics

28

29

30

31 **Abstract** (149 words)

32

33 Increasing interest in deubiquitinases (DUBs) and ubiquitin E3 ligases as drug targets to  
34 modulate critical molecular pathways in disease is driven by the discovery of specific cellular  
35 roles of these enzymes. Key to this is the identification of DUB or E3 ligase substrates. While  
36 global cellular ubiquitination changes upon perturbation of DUB/E3 ligase activity can be  
37 studied using mass spectrometry-based proteomic methods, these datasets include indirect  
38 and downstream ubiquitination events. To enrich for direct substrates of DUB/E3 ligase  
39 enzymes, we have combined proximity-labelling methodology (APEX2) and subsequent  
40 ubiquitination enrichment (based on the K- $\epsilon$ -GG motif) to form a proximal-ubiquitome  
41 workflow. We have applied this technology to identify altered ubiquitination events in the  
42 proximity of the DUB ubiquitin specific protease 30 (USP30) upon its inhibition. We show  
43 ubiquitination events previously linked to USP30 on TOMM20 and FKBP8 and the previously  
44 undescribed candidate substrate LETM1, which is deubiquitinated in a USP30-dependent  
45 manner.

46

47

48

49

50

51

52

53

54

55

56

57

58

59

60

61

## 62 Introduction

63

64 Ubiquitin (Ub) constitutes a highly conserved protein found across all eukaryotic organisms.<sup>1</sup>

65 Ub can be activated and covalently attached to a target protein via the successive action of  
66 E1, E2, and E3 enzymes, forming a cascade that culminates in a post-translational  
67 modification. This intricate process plays an instrumental role in a myriad of cellular functions,  
68 encompassing protein homeostasis, signal transduction, DNA replication, and transcriptional  
69 regulation.<sup>2</sup>

70

71 E3 ligases and deubiquitinating proteases (DUBs) are specialist enzymes that add and remove  
72 covalent ubiquitin modifications to and from target substrates. Both enzyme families are  
73 essential in the maintenance of Ub homeostasis. This dynamic balance is integral to normal  
74 cellular operation, and can alter the fate of Ub-modified proteins.<sup>3</sup> Imbalances in the  
75 ubiquitination of proteins have been implicated in various pathological conditions, including  
76 cancer and neurodegenerative diseases.<sup>4,5</sup> Therefore, the identification of E3 ligase/DUB  
77 substrates not only enriches our understanding of their biological roles but also opens  
78 avenues for the exploration of these enzymes as potential therapeutic targets.<sup>6</sup>

79

80 Several methodologies have been previously employed to identify potential substrates of E3  
81 ligases that could also be translated to identify DUB substrates. One category involves fusion  
82 techniques, such as UBAITS,<sup>7</sup> TULIP,<sup>8</sup> and TULIP2,<sup>9</sup> which use overexpressed Ub-E3 ligase  
83 fusions to trap and purify ligase-substrate adducts, often under denaturing conditions.  
84 Another category includes *in vitro* techniques such as E2-dID, orthogonal Ub transfer  
85 (OUT),<sup>10,11</sup> and microarray assays, which employ engineered enzymes or biotin-labeled Ub  
86 conjugates to target specific substrates. Finally, UbPOD<sup>12</sup> and BioE3<sup>13</sup> are approaches that use  
87 tagged ubiquitin as a biotinylation substrate for an E3 ligase conjugated to a proximity  
88 labelling enzyme. While no single method is universally applicable, each has proven effective  
89 for discovering substrates for specific E3 ligases.

90

91 While these methods enrich for interactors of E3 ligases, they do not provide information on  
92 the ubiquitination sites on these potential substrates. The identification of specific

93 ubiquitination/deubiquitination sites is critical for interpreting the biological meaning of the  
94 ubiquitination events altered by an E3 ligase/DUB, and for utilising the ubiquitination site as  
95 a biomarker in the case that an E3 ligase/DUB is therapeutically targeted. Additionally, altered  
96 ubiquitination states on proteins that are E3 ligase/DUB interactors increases the confidence  
97 that these hits may be direct substrates.

98

99 Among the most established approaches to identify ubiquitin sites is the enrichment of the  
100 Ubiquitin Remnant Motif (K- $\epsilon$ -GG) left behind at the sites of lysine ubiquitination after protein  
101 trypsinization, followed by immunoprecipitation and subsequent mass spectrometry  
102 analysis.<sup>14,15</sup> The application of targeted knockouts, catalytically inactive mutants or of  
103 specific small molecule inhibitors, in conjunction with the K- $\epsilon$ -GG technique, can accelerate  
104 the identification process of DUB or E3 ligase substrates from specific alterations observed in  
105 the cellular ubiquitome.

106

107 However, the K- $\epsilon$ -GG method comes with limitations. One notable drawback is that many  
108 altered ubiquitination events may result from downstream secondary effects upon the  
109 reduced activity of a DUB or E3 ligase. Whilst these events are of interest, they are not all  
110 reflective of direct enzyme substrates and activity.

111 In the last decade, innovative proximity labelling approaches, such as BioID<sup>16</sup> and APEX<sup>17</sup>,  
112 have been developed to enhance the identification of proteins within the micro-environment  
113 of a protein of interest. Proximity labelling has previously been successfully integrated with  
114 phospho-enrichment strategies to investigate spatially referenced proximity  
115 phosphoproteomics.<sup>18–20</sup> In this study, we show that the effective combination of proximity  
116 labelling followed by post-translational modification enrichment can also be applied to the  
117 study of ubiquitination. This allows for the capture of protein ubiquitination states that are  
118 specifically localised to DUBs/E3 ligases. Application of the technique has the potential to  
119 enhance the resolution and accuracy of substrate identification of a DUB or E3 ligase upon  
120 the perturbation of its activity.

121

122 Ascorbate peroxidase-2 (APEX2) was considered favourable as a proximity labelling enzyme  
123 for this methodology due to the speed of the biotinylation reaction occurring on the second  
124 timescale. This labelling snapshot enables the capture of an acute cellular protein

125 ubiquitylation profile upon DUB inhibition/genetic depletion, without time-dependent  
126 convolution from the dynamic ubiquitination process. Additionally, APEX2 favours the  
127 biotinylation of tyrosine residues, meaning that it does not interfere with ubiquitination  
128 events occurring on lysine residues. Other proximity labelling approaches, such as BioID and  
129 TurboID, should not be applied to this methodology due to the long timescale of the labelling  
130 reaction and the biotinylation of lysine residues.

131

132 USP30 was selected as a model DUB for the development of this methodology due to its  
133 potential as a drug target, with the knockout of USP30 resulting in increased turnover of  
134 mitochondria via mitophagy.<sup>21</sup> The process of mitophagy could be targeted for multiple  
135 therapeutic applications, such as for the treatment of Parkinson's disease.<sup>21,22</sup> Therefore,  
136 further insight into the role USP30 plays in the process of mitophagy, and potential  
137 biomarkers resulting from its inhibition are highly relevant. Additionally, previous  
138 characterisation of the outer mitochondrial membrane (OMM) localisation of USP30, and  
139 ubiquitomics studies of the activity of USP30 enable cross-validation of the proximal-  
140 ubiquitome of USP30 to existing datasets.<sup>22-24</sup>

141

142 Here, we present the development of a novel workflow, combining highly sensitivity APEX2  
143 proximity labelling with a subsequent K-ε-GG immunoprecipitation to elucidate the proximal-  
144 ubiquitome of a target DUB (USP30), both in the presence and absence of an USP30 inhibitor,  
145 compound '39', a previously described potent, cell permeable, and selective USP30  
146 inhibitor.<sup>25-27</sup> The proximal-ubiquitomics methodology gives a unique insight into the role of  
147 the USP30 in process of mitophagy. Potential direct USP30 substrates are uncovered through  
148 the application of the methodology, and subsequent validation provides evidence for USP30  
149 enacting on the ubiquitination state of proteins considered critical to mitochondrial function  
150 and turnover. We focus on validating a novel previously undescribed potential USP30  
151 substrate – leucine-containing zipper and EF-hand transmembrane protein 1 (LETM1), an  
152 essential protein described to be involved in various critical functions, including mitochondrial  
153 ion transport, regulation of mitochondrial volume, energy metabolism, and maintenance of  
154 mitochondrial morphology.<sup>28-31</sup>

155

## 156 **Results**

157

### 158 **Proximal-ubiquitomic methodology optimization**

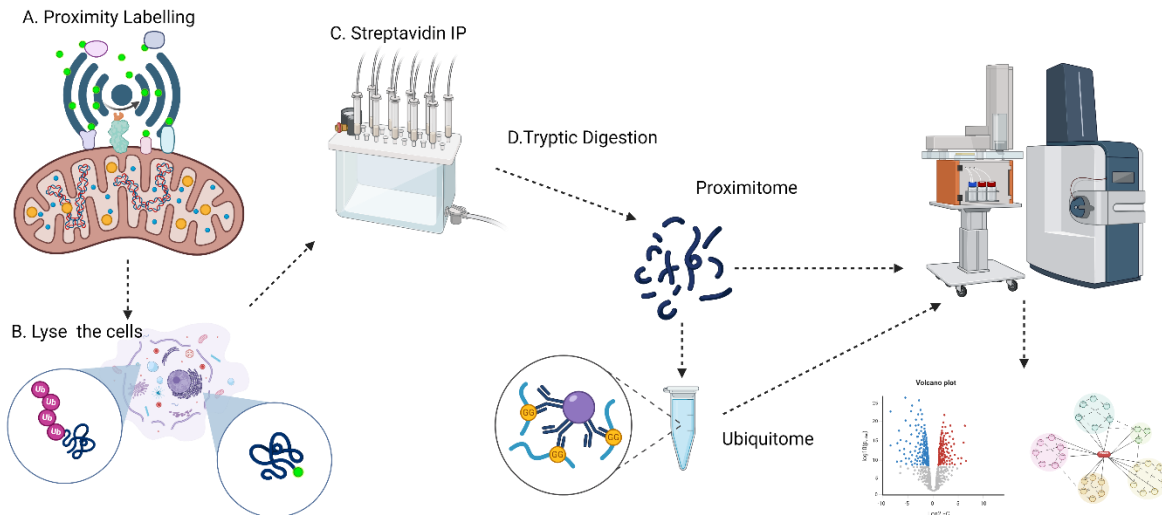
159

160 Each aspect of the workflow applied in Figure 1 was optimised to ensure efficient capture of  
161 ubiquitylated proteins in the proximity of USP30 (Figure 2a). This is critical for the adaptation  
162 of the methodology to different systems. In this model USP30-APEX2 system, the conjugated  
163 enzymes were stably expressed in HEK293 cells with a low expression promoter (PGK).<sup>32</sup> We  
164 observed a moderate 3.8-fold increase in USP30 expression as compared to that of its  
165 endogenous expression levels (Figure 2b & S1a). Maintained USP30 activity was confirmed  
166 using a DUB activity-based probe (ABP), consisting of ubiquitin with a propargylamine  
167 warhead and a haemagglutinin tag (HA-Ub-PA). The ~10 kDa molecular weight increase of  
168 USP30-APEX2 in the presence of HA-Ub-PA indicates that the active site of USP30 is still able  
169 to bind ubiquitin and the active site cysteine is still reactive (Figure 2c & S1a). This ABP is  
170 broadly reactive with the majority of cysteine-active DUBs, and so can be used to check  
171 retained activity if the proximal-ubiquitomics methodology is applied to other DUBs.<sup>33</sup> The  
172 maintained localization of USP30-APEX2 to the OMM was confirmed via TOMM20 co-  
173 localisation microscopy (Figure 2d) and digitonin membrane isolation (Figure S1b).

174

175 After confirming that the properties of the DUB-APEX2 conjugate are reflective of the  
176 endogenous DUB, the APEX2 biotinylation labelling efficiency was optimised, to maximise the  
177 capture of proximal proteins. Incubating cells with a concentration range of biotin  
178 demonstrated that a minimum of 5 mM biotin was necessary for efficient protein  
179 biotinylation (Figure 2e). In previous studies, biotin incubation with cells was performed for  
180 30 minutes at 37 °C with increased incubation not resulting in increased labelling, indicating  
181 the incubation time is sufficient for full dispersal of the biotin throughout the cells.<sup>34</sup> With  
182 the maximal biotinylation conditions, the volume of streptavidin beads then needs to be  
183 optimised to achieve efficient capture of all biotinylated proteins. By assessing the input,  
184 flow-through and elution of the biotin streptavidin pull down, we maximised the capture  
185 capacity of the streptavidin beads for this system with 1 mL of beads / 10 mg of input protein  
186 (Figure 2f).

187



188  
189  
190  
191  
192  
193  
194  
195

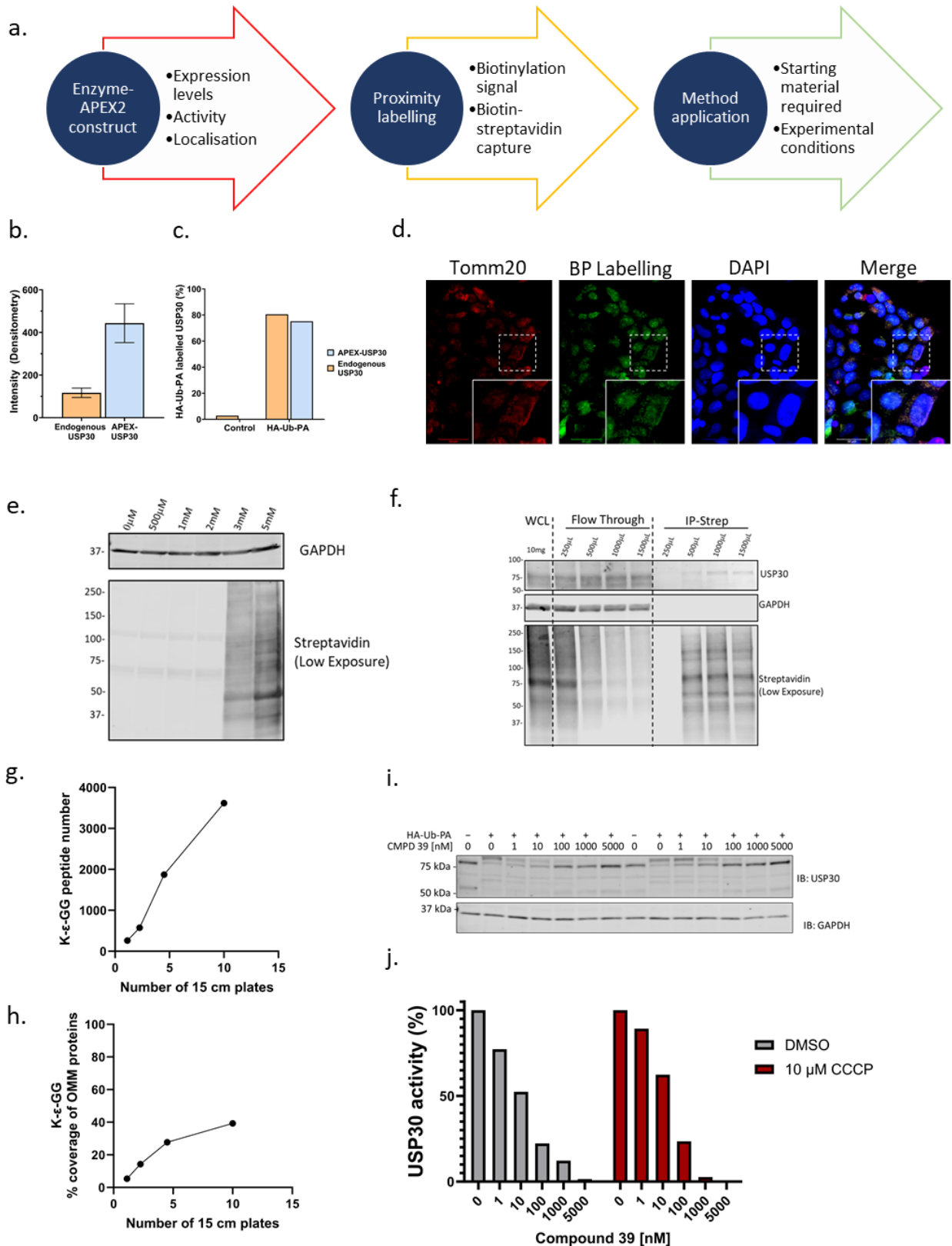
**Figure 1 | Integrated proximal-ubiquitomics methodology workflow.** Proximity labelling biotinylates the microenvironment of a DUB/E3 ligase of interest. The biotinylated proteins are then pulled down with streptavidin on the protein level to encompass ubiquitination events proximal to the biotinylation site. Biotinylated proteins are then digested with trypsin and ubiquitination events are enriched using a K-ε-GG antibody. Ubiquitylated proteins from the proximity of the enzyme of interest are then quantified by LC-MS/MS. Figure created using [www.biorender.com](http://www.biorender.com).

196 Once proteins proximal to USP30 were biotinylated by APEX2 and pulled down using  
197 streptavidin, the ubiquitination sites of these proteins were enriched for LC-MS/MS  
198 identification. This was achieved by trypsinizing the proteins and immunoprecipitating the K-  
199 ε-GG remnant motif that remains after the trypsinization of proteins reflecting ubiquitination,  
200 Neddylaton or ISGylation sites. However, under most normal physiological conditions, the  
201 source of the majority of K-ε-GG remnant sites is ubiquitination (>94 %).<sup>35</sup> Without K-ε-GG  
202 pulldown, we did not detect ubiquitination sites in the USP30 proximity labelling (data not  
203 shown), justifying the necessity for a subsequent enrichment step. The recommended  
204 amount of protein material for K-ε-GG enrichment is 1-2 mg.

205

206 Measurement of protein/peptide levels is challenging in the workflow due to interference  
207 from the presence of anti-oxidants in the lysis buffer. Additionally, proteins such as  
208 streptavidin and trypsin obscure the absolute protein quantitation after biotinylation elution  
209 and the peptide quantitation prior to the K-ε-GG enrichment, respectively. Therefore,  
210 material for this experimentation was optimised for the system based on the number of 15  
211 cm plates at confluence used as starting material. When performing K-ε-GG enrichments  
212 without proximity enrichment the number of identified K-ε-GG sites identified

213



214 **Figure 2 | Optimization workflow for the proximal-ubiquitomics methodology.** **a.** Scheme of experimental  
 215 optimization strategy. **b.** Densitometric intensity of HEK293 endogenous USP30 and APEX2-USP30 (N=3  
 216 quantification of separate bands from 1 sample). **c.** Percentage of endogenous and APEX2 conjugated USP30  
 217 labelled by HA-Ub-PA. **d.** Immunofluorescence of TOMM20, biotin-phenol (BP) and DAPI staining after USP30-  
 218 APEX2 biotinylation in HEK293 cells. **e.** Biotin-phenol concentration dependence of USP30-APEX2 biotinylation  
 219 in HEK293 cells. **f.** Streptavidin pulldown optimization after USP30-APEX2 biotinylation with 5 mM biotin-

220 phenol. **g.** Number of GlyGly peptides identified from the proximal-ubiquitomics methodology with different  
221 amounts of input material. **h.** Percentage of outer mitochondrial membrane (OMM) Mitocarta 3.0 proteins  
222 identified from the proximal-ubiquitomics methodology with different amounts of input material. **i.** HA-Ub-PA  
223 labelled USP30-APEX after a 6hr incubation of the USP30-APEX2 HEK293 cells with the indicated concentration  
224 of compound **39**, with and without 10  $\mu$ M CCCP. **j.** Normalised densitometric quantification of USP30-APEX2  
225 HA-Ub-PA labelling and inhibition after a 6hr incubation of the USP30-APEX2 HEK293 cells with the indicated  
226 concentration of compound **39**, with and without 10  $\mu$ M CCCP.

227

228 can vary greatly, depending on the source material, experimental conditions and mass-  
229 spectrometry methodology applied.<sup>36,37</sup>

230

231 In the case of the proximal-ubiquitomics workflow presented here, we saw a linear increase  
232 in the number of K- $\epsilon$ -GG sites with increasing input material, up to 4000 sites with 10 x 15 cm  
233 plates (Figure 2g). However, the coverage of OMM localised proteins that were identified as  
234 ubiquitinated begins to plateau between 5 - 10 x 15 cm dishes of input material (Figure 2h).  
235 Thus, 5 x 15 cm dishes per condition were selected as the optimal input material for this  
236 system to capture ubiquitination events proximal to USP30. The abundance of USP30 has  
237 been reported to be in the bottom 10 % of ~8000 proteins identified in a HEK293 proteome  
238 (PaxDB 5.0).<sup>38,39</sup> With the use of a low expression promotor to mimic endogenous USP30  
239 levels in this study, large amounts of input material were required for this model system. This  
240 may vary depending on expression levels of the protein of interest, and subsequently the  
241 amount of material recovered post streptavidin IP.

242

243 After optimization of the USP30-APEX2 system and proximal-ubiquitomics workflow,  
244 experimental conditions to elucidate potential USP30 substrates using compound **39** were  
245 optimized. To maximize ubiquitination events in the proximity of USP30, cells were treated  
246 with CCCP to depolarize the mitochondria and subsequently activate the PINK1/Parkin S65  
247 phospho-ubiquitination pathway. Mitochondrial depolarization conditions have previously  
248 been shown to reveal increased OMM protein ubiquitination events as a consequence of  
249 USP30 knockout.<sup>24</sup> In this HEK293 USP30-APEX2 system, maximal S65 phospho-ubiquitin was  
250 identified with 10  $\mu$ M of CCCP cell treatment after 6 hours of incubation (Figure S1c).

251

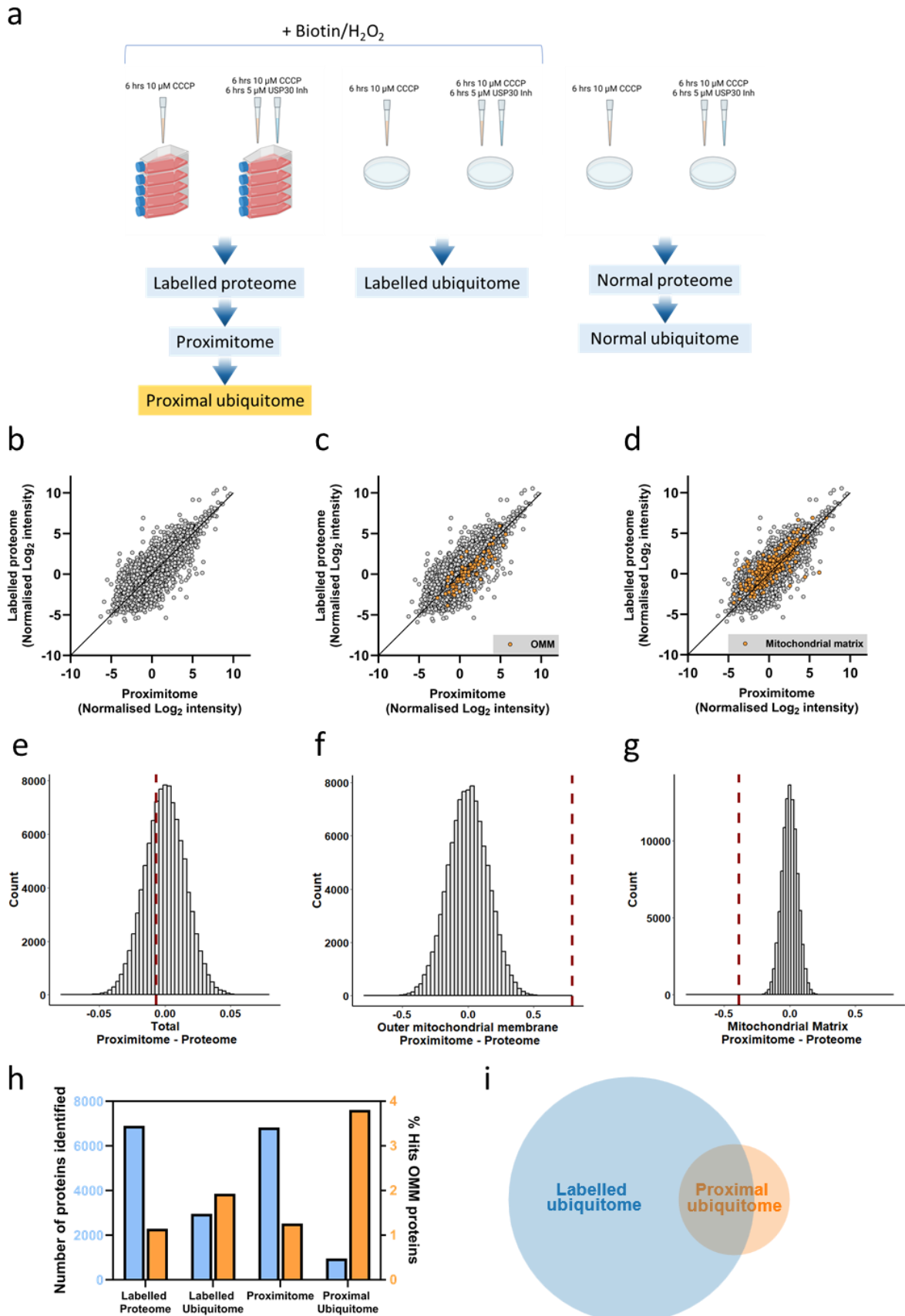
252 The concentration of the small molecule compound **39** required for complete USP30  
253 inhibition in the USP30-APEX2 overexpression system was assessed using the HA-Ub-PA ABP.  
254 After 6 hours of cellular incubation, full inhibition of HA-Ub-PA binding to USP30-APEX2 was

255 identified with 5  $\mu$ M of compound **39**, regardless of the presence of 10  $\mu$ M CCCP (Figure 2i-j).  
256 From this optimization, 10  $\mu$ M CCCP treatment +/- 5  $\mu$ M of compound **39** was applied to  
257 identify acute ubiquitination events proximal to USP30 occurring as a consequence of USP30  
258 inhibition on mitochondria undergoing the process of mitophagy.

### 259 **Optimised protocol reveals USP30 proximal ubiquitome enriched for OMM**

260  
261 The two conditions (CCCP treatment +/- 5  $\mu$ M of compound **39**) were repeated in  
262 quadruplicate, with 5 x T175 flasks pooled per replicate. APEX2 biotin labelling was catalysed  
263 by the addition of H<sub>2</sub>O<sub>2</sub> and quenched with multiple antioxidant washes. After lysis 5 % were  
264 taken for the 'labelled proteome', with the remaining material used as input for the biotin-  
265 streptavidin pulldown. Equal input and eluate levels for each streptavidin pulldown were  
266 checked by western blot (Figure S1d). From this pull down, 10 % of eluates were taken for the  
267 'proximitome' and the remaining material was trypsinized and used as input for the K- $\epsilon$ -GG  
268 immunoprecipitation, forming the 'proximal-ubiquitome' (Figure 3a). Each step represents  
269 important information about the effect of USP30 inhibition as well as providing normalisation  
270 data to ensure ubiquitination events are not altered as a consequence of perturbed protein  
271 abundance or protein proximity to USP30 with compound **39** treatment.

272  
273 To compare the method of the proximal-ubiquitome to the classical ubiquitomics workflow  
274 we included a 'labelled ubiquitome' (N=3) with APEX2 biotinylation protein labelling, but  
275 without biotin enrichment by streptavidin. This allowed for the comparison of ubiquitination  
276 events occurring in the whole cell with those occurring in the proximity of USP30 in the same  
277 system. We also included a control proteome and ubiquitome (N=4) without APEX2  
278 biotinylation labelling ('normal proteome' and 'normal ubiquitome'), to assess the effect of  
279 the biotin/H<sub>2</sub>O<sub>2</sub> treatment and subsequent APEX2 biotinylation reaction on protein and  
280 ubiquitination site identification/quantification (Figure 3a). The Log<sub>2</sub> intensities for all  
281 datasets averaged coefficients of variations (CVs) below 10 %. The raw intensities showed  
282 higher CVs for the ubiquitomes compared to the proximitome/proteomes, with CVs for the  
283 proximal-ubiquitome comparable to the control ubiquitomes (Figure S2 a-f). Principal  
284 component analysis showed clustering of replicates based on presence or absence of USP30  
285 inhibition (Figure S2 g-i).



286  
287  
288

**Figure 3 | USP30 proximal ubiquitome enriched for outer mitochondrial membrane (OMM) proteins. a.** Experimental design to compare the proximal ubiquitome of USP30 +/- compound 39, with its corresponding

289 proximitome, proteome and ubiquitome. A control proteome and ubiquitome without APEX2 biotin labelling  
290 were also included for comparison. **b-d.** The averaged Log<sub>2</sub> intensity of proteins quantified in the proximitome  
291 vs proteome (with APEX2 biotinylation and CCCP treatment) with Mitocarta 3.0 annotated OMM proteins or  
292 MM proteins in orange. **e-g.** Permutation analysis – the dotted red line denotes the average of the X-Y intensity  
293 differences between the proximitome and the proteome of all proteins, outer mitochondrial membrane (OMM)  
294 proteins and mitochondrial membrane (MM) proteins. The distribution shows the randomized averages of these  
295 values over 100,000 permutations. **h.** The number of proteins identified in the biotin labelled proteome, labelled  
296 ubiquitome, proximitome and proximal ubiquitome vs. the % of Mitocarta 3.0 OMM annotated proteins. **i.** The  
297 overlap in K-ε-GG peptides identified in the labelled ubiquitome and proximal ubiquitome.

298

299 To examine the effect of APEX2 biotin labelling on the proteome and ubiquitome of USP30-  
300 APEX2 expressing HEK293 cells, the labelled proteome was compared to the normal  
301 proteome, and the labelled ubiquitome was compared to the normal ubiquitome. There were  
302 significant changes to the intensity of proteins identified in the proteomes (Figure S3a), with  
303 String analysis<sup>40</sup> identifying that the majority of proteins with significantly increased  
304 intensities upon APEX2 labelling are structural constituents of chromatin (Figure S3b). This  
305 may be attributable protein upregulation in response to DNA damage caused by the H<sub>2</sub>O<sub>2</sub>  
306 treatment<sup>41</sup> during the APEX2 labelling. No Mitocarta 3.0 annotated proteins were altered,  
307 indicating that the labelling of proteins with biotin does not affect the detection and intensity  
308 of the proteins anticipated to be proximal to USP30. There were also significant changes to  
309 the intensity of K-ε-GG peptides identified in the labelled ubiquitome when compared to the  
310 normal ubiquitome, including peptides originating from Mitocarta 3.0 annotated proteins  
311 (Figure S3c). The altered ubiquitome as a consequence of APEX2 catalysed H<sub>2</sub>O<sub>2</sub> biotin  
312 labelling is a limitation of proximity labelling and highlights the importance of subsequent  
313 validation of hits identified with proximal-ubiquitomics in systems lacking APEX2 biotinylation  
314 process.

315

316 Proximity-labelling of USP30-APEX2 has a high background due to its exposure to a vast  
317 number of cytoplasmic proteins and the large number of proteins that bind as background  
318 during the streptavidin pull-down. However, proteins that are most frequently proximal to  
319 USP30 will include genuine USP30 interactors, and therefore potential substrates of USP30.  
320 OMM proteins are a key example of this, with the fixed positioning of these proteins likely to  
321 increase their USP30-APEX2 biotinylation frequency, and consequently their LC-MS/MS  
322 intensities. Additionally, previously identified USP30 dependent ubiquitylation events are  
323 localised to the OMM, such as TOMM20.<sup>22,24,42,43</sup> To ensure the successful enrichment of  
324 proteins proximal to USP30-APEX2, the intensity of proteins annotated in Mitocarta3.0 as

325 OMM vs mitochondrial matrix (MM) proteins were compared in the labelled proteome vs the  
326 proximitome (Figure 3b-d).

327

328 Permutation calculations were used to randomize the difference in X-Y scatter points in Figure  
329 3b with the distribution of the average differences of the permutations plotted in Figure 3e.  
330 Here, the average difference in X-Y coordinates denoted by the red dashed line is within the  
331 normal distribution of the permutations, showing that the identified proteins are comparably  
332 intense between the proximitome and labelled proteome overall. When the same  
333 calculations are performed for the Mitocarta 3.0 annotated OMM proteins (Figure 3c-f) and  
334 MM proteins (Figure 3d-g), the average differences denoted by the red dashed line are  
335 significantly distinct from the randomized normal distribution, with the average difference  
336 never occurring in 100,000 permutations. These calculations show an enrichment of OMM  
337 proteins, and a reduction of MM proteins in the proximitome when compared to the labelled  
338 proteome. This confirms that the proximitome represents an enrichment of proteins that are  
339 situated within the proximity of USP30.

340

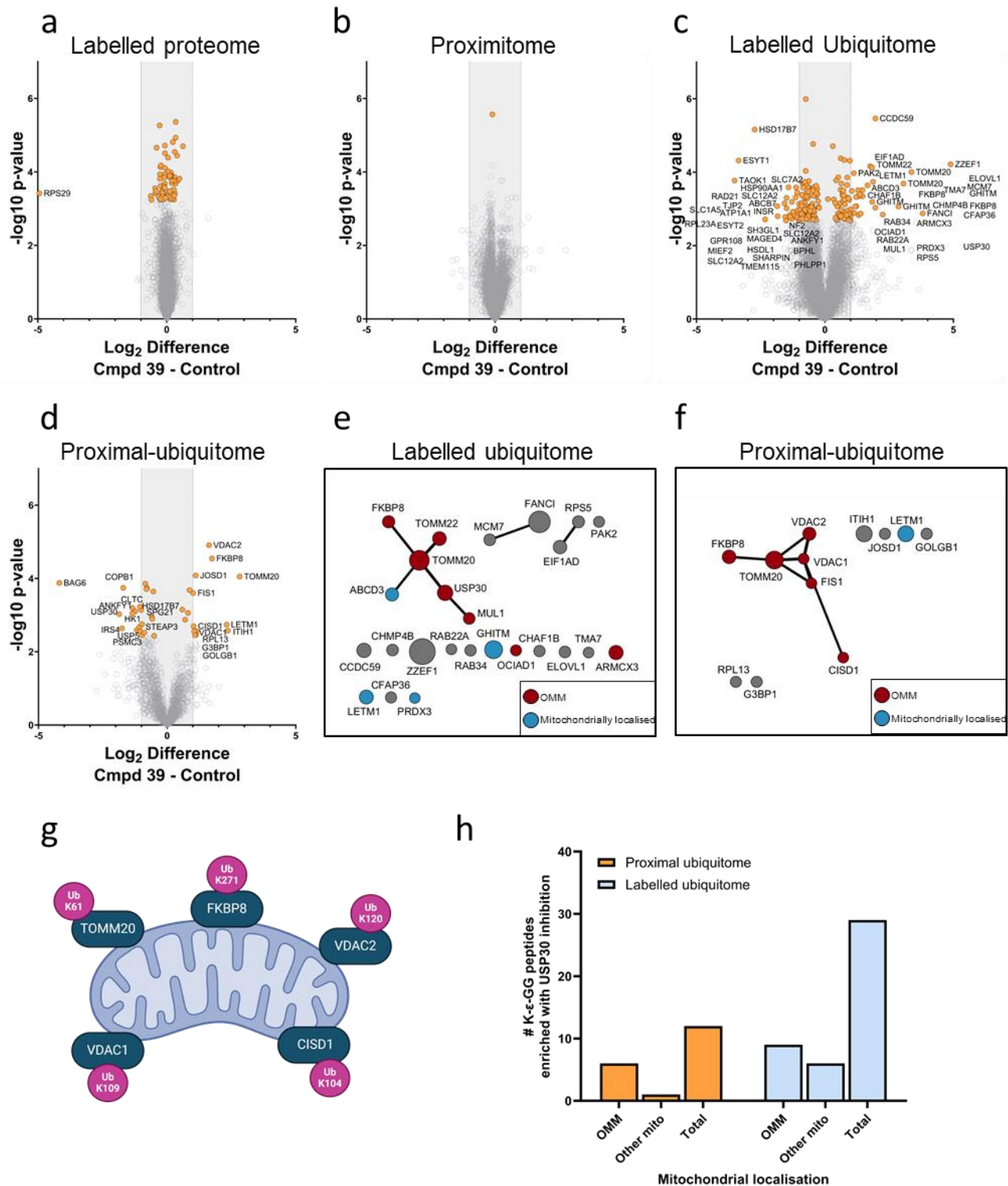
341 The enrichment of OMM proteins in the proximitome of USP30-APEX2 also translates through  
342 to the proximal-ubiquitome of the protein. The percentage of proteins linked to the OMM  
343 based on Mitocarta3.0 annotation is doubled in the proximal-ubiquitome compared to the  
344 control labelled ubiquitome (Figure 3h). Despite a reduced number of K-ε-GG modified  
345 peptides identified in the proximal-ubiquitome compared to the labelled ubiquitome, over 30  
346 % of proximal-ubiquitome peptides were not identified in the labelled ubiquitome (Figure 3i).  
347 This indicates that proximal-ubiquitomics in this system enriches for a subset of ubiquitination  
348 events from the proximity of USP30, thus narrowing down potential substrates of the DUB.

349

### 350 **Application of proximal-ubiquitomics to identify novel substrates of USP30**

351

352 Following the experimental outline in Figure 3a, the labelled proteome and the proximitome  
353 were assessed for protein intensity alterations occurring as a consequence of USP30  
354 inhibition (Figure 4a-b). Although some proteins were significant in their alterations (denoted  
355 in orange), only 1 protein in the labelled proteome and no proteins in the proximitome were



356 **Figure 4 | Discovery of USP30 substrate candidates by integrated proximal ubiquitomics** **a.** Labeled  
 357 proteome volcano plot showing the effect of compound **39** treatment on protein levels in CCCP treated  
 358 HEK293 USP30-APEX2 cells with APEX2 biotin labelling. **b.** Proximitome volcano plot showing the effect of  
 359 compound **39** treatment on protein levels captured from streptavidin pull-down after USP30-APEX2  
 360 biotinylation in CCCP treated HEK293 USP30-APEX2 cells. **c.** Labeled ubiquitome volcano plot showing the  
 361 effect of compound **39** treatment on peptides with K-ε-GG sites after K-ε-GG peptide enrichment in CCCP  
 362 treated HEK293 USP30-APEX2 cells with USP30-APEX2 biotin labelling. **d.** Proximal-ubiquitome volcano plot  
 363 showing the effect of compound **39** treatment on peptides with K-ε-GG sites after streptavidin pull-down of  
 364 USP30-APEX2 biotinylated proteins followed by K-ε-GG peptide enrichment in CCCP treated HEK293 USP30-

365 APEX2 cells. **e-f.** Cytoscape string analysis of K- $\epsilon$ -GG peptides that are significantly increased upon compound  
366 **39** treatment in CCCP treated HEK293 USP30-APEX2 cells in the labelled ubiquitome (**e**) and proximal  
367 ubiquitome (**f**). Circle size is proportional to the Log<sub>2</sub> difference in K- $\epsilon$ -GG peptide intensity +/- compound **39**  
368 treatment, with the largest difference used if multiple peptides originate from the same protein. Red circles  
369 denote OMM and blue circles denote other mitochondrially localised Mitocarta 3.0 annotated proteins.  
370 Cytoscape String network based off string confidence score cut off  $\geq 0.7$ . Edge width is proportional to string  
371 confidence score.<sup>40,44</sup> **g.** K- $\epsilon$ -GG sites of the 5 proximal ubiquitome hits that overlap with altered ubiquitination  
372 states of proteins with USP30 inhibition/KO reported by Jones *et al.*<sup>22</sup> and Ordureau *et al.*<sup>24</sup> **h.** Number of K- $\epsilon$ -  
373 GG peptides identified in the proximal ubiquitome and labelled ubiquitome either in total, with OMM  
374 localisation or with other mitochondrial localisation annotation ('other mito') with Mitocarta 3.0 annotation.  
375

376 increased or decreased more than a Log<sub>2</sub> fold change  $> 1$  with USP30 inhibition. Minimal  
377 changes to the proteome as a consequence of USP30 inhibition or knockout have also been  
378 previously reported in the literature.<sup>22,42</sup>

379  
380 Whilst proteins identified in the labelled proteome and USP30 proximitome were not  
381 perturbed upon USP30 inhibition, significant alterations to ubiquitinated peptide intensities  
382 as a consequence of USP30 inhibition were observed in the labelled ubiquitome and proximal-  
383 ubiquitome (Figure 4c-d). Significant increases in the intensity of ubiquitinated peptides with  
384 USP30 inhibition represent potential USP30 substrates. Here, significantly increased  
385 ubiquitination ( $> 1$  log<sub>2</sub> difference) is detected at various sites on 32 different proteins across  
386 the labelled ubiquitome and proximal ubiquitome (Figure 4e-f). Of the 32 proteins, 5 overlap  
387 between this dataset and two previously reported datasets with significantly increased  
388 ubiquitination events in the case of USP30 knockout in depolarizing conditions.<sup>22,24</sup> Those hits  
389 include TOMM20, FKBP8, VDAC2, VDAC1 and CISD1, all of which are Mitocarta3.0 annotated  
390 as OMM proteins. Of the 5 hits, 2 are detected as significantly increased with USP30 inhibition  
391 in the labelled ubiquitome out of 25 in total. All 5 are detected as significantly increased with  
392 USP30 inhibition in the proximal-ubiquitome out of 12 proteins in total (Figure 4g), indicative  
393 of the ability of the proximal-ubiquitomics technique to detect robust alterations occurring  
394 as a consequence of a reduction in USP30 activity across different cell types and experimental  
395 conditions.

396  
397 The total number of increased ubiquitylation events as a consequence of USP30 inhibition is  
398 substantially reduced in the proximal-ubiquitome when compared to the labelled  
399 ubiquitome. A greater proportion of increased ubiquitylation events are OMM in the

400 proximal-ubiquitome when compared to the labelled ubiquitome, whereas a smaller  
401 proportion of ubiquitylation events are occurring on proteins associated with other parts of  
402 the mitochondria (Figure 4h). This finding is reflective of the enrichment of OMM proteins in  
403 the proximitome relative to the proteome, and demonstrates that the proximal-ubiquitomics  
404 methodology is enabling the detection of changes in ubiquitination events occurring in the  
405 proximity of USP30.

406

#### 407 **LETM1 is a USP30 interactor and substrate**

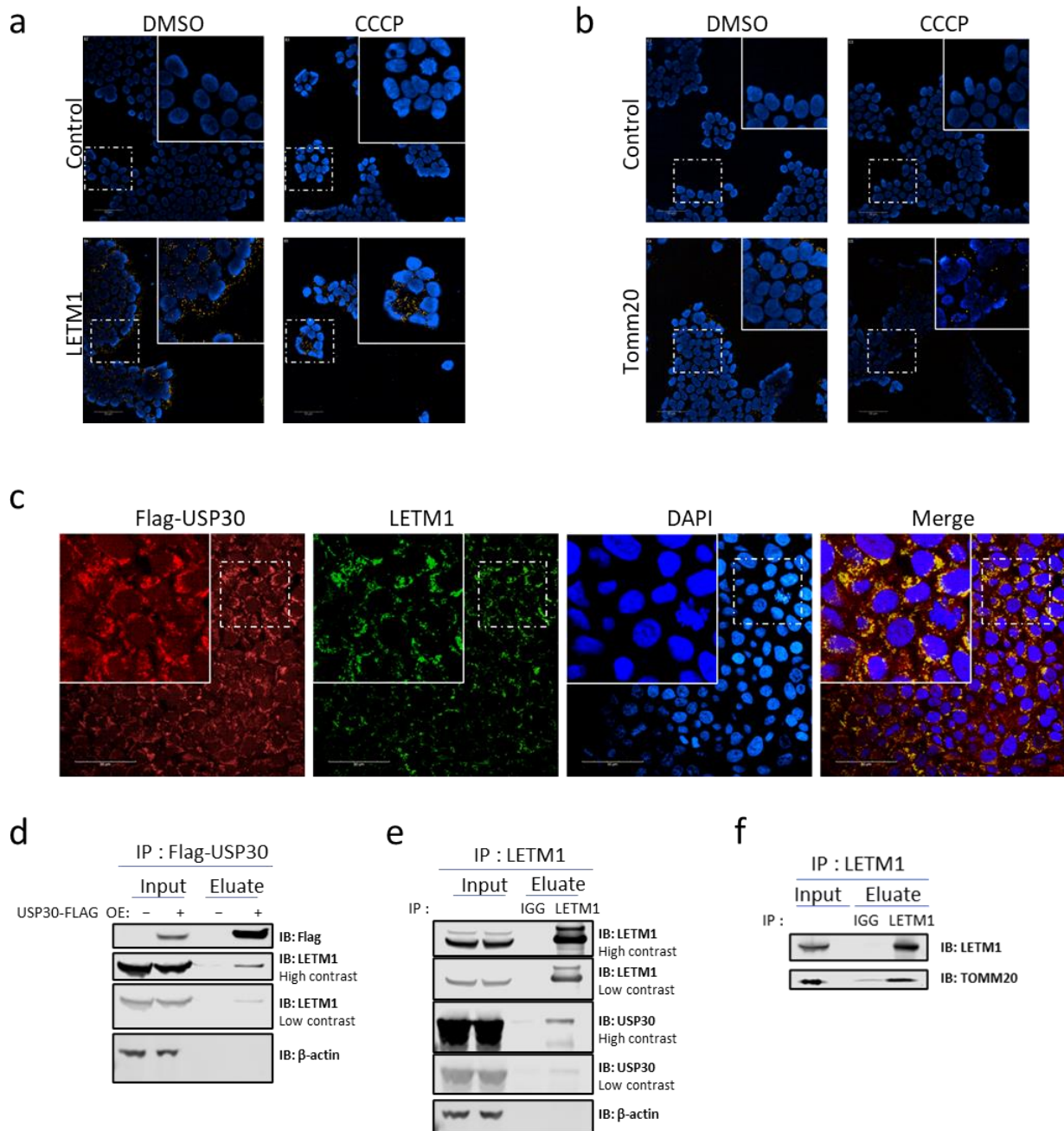
408

409 The increase in ubiquitination of OMM proteins with USP30 inhibition in the proximal-  
410 ubiquitome has also been previously reported with USP30 KO.<sup>24</sup> However, the increased  
411 ubiquitination of the inner mitochondrial membrane (IMM) protein LETM1 as a consequence  
412 of reduced USP30 activity has not previously been reported to our knowledge. The increase  
413 in LETM1 ubiquitination with USP30 inhibition was identified in both the 'labelled ubiquitome'  
414 and 'proximal-ubiquitome', and so LETM1 was further investigated as a potential USP30  
415 substrate.

416

417 Initially, we sought to validate the proximity of USP30 to LETM1 using antibody-based  
418 proximity ligation assays (PLA), allowing for the detection of proteins within a 30-40 nm  
419 proximity via fluorescence. In the absence of a selective USP30 antibody suitable for  
420 immunofluorescence (IF) / immunoprecipitation (IP), Flag-USP30 was overexpressed, and PLA  
421 was performed both with and without CCCP. A strong PLA signal confirmed that endogenous  
422 LETM1 and Flag-USP30 are in proximity regardless of the presence of CCCP (Figure 5a). USP30  
423 has previously been found to Co-IP with TOMM20,<sup>42</sup> and the increased ubiquitination of  
424 TOMM20 with USP30 KO in ubiquitomic experiments has previously been validated by  
425 western blot.<sup>22,24</sup> Therefore, TOMM20 was included as a positive control in experiments  
426 investigating LETM1 as a substrate of USP30. Here, endogenous TOMM20 was also identified  
427 as proximal to exogenous Flag-USP30 by PLA assays, indicating that the exogenous Flag-  
428 USP30 was correctly located on the mitochondria, and co-localised to the TOMM complex  
429 (Figure 5b).

430



431 **Figure 5 | LETM1 as USP30 interactor.** **a-b** Proximity Ligation Assay (PLA) in HEK293 cells. HEK293 cells  
 432 transiently transfected with Flag-USP30, with PLA reaction between anti-Flag antibody and anti-LETM1 antibody  
 433 **(a)** or an anti-Tomm20 antibody **(b)**. Yellow punctate signals represent the reported interactions, and blue  
 434 signals indicate nuclei. A single antibody control (None) was included. Scale bar: 10 μm. **c** Confocal images of  
 435 HEK293 cells +/- CCCP transiently expressing Flag-USP30 and endogenous LETM1 protein. Anti-Flag antibody  
 436 (red), anti-LETM1 antibody (green), and DAPI (blue) for nuclei visualization. Scale bars: 10 μm. **d-e** HEK293T cells  
 437 transiently expressing Flag-USP30 **(d)** USP30 was pulled down using an anti-Flag antibody **(e)** LETM1 was pulled  
 438 down using an anti-LETM1 antibody **(f)** SH-SY5Y cell LETM1 pull down using anti-LETM1 antibody.

439 To further explore and increase our confidence regarding the proximity of USP30 to LETM1,  
 440 a co-localization experiment was performed. Flag-USP30 was overexpressed and  
 441 colocalization with endogenous LETM1 was assessed. Endogenous LETM1 and Flag-USP30  
 442 colocalized, supporting the possibility that these two proteins could be in the same protein

443 complex in the presence of CCCP (Figure 5c). To strengthen the validity of our colocalization  
444 findings, we calculated Li's Intensity Correlation Quotient (ICQ) to quantify the degree of  
445 correlation between LETM1 and USP30 signals, resulting in a value of 0.182, which is  
446 indicative of a positive correlation. The USP30-LETM1 localisation in the presence of CCCP  
447 was further validated with Co-IP experiments, where the pulldown of exogenous Flag-USP30  
448 captured endogenous LETM1, and the pull down of endogenous LETM1 captured exogenous  
449 Flag-USP30 (Figure 5d-e).

450

451 Additionally, Co-IP successfully captured endogenous TOMM20 where endogenous LETM1  
452 was pulled down (Figure 5f). These data collectively support that LETM1 and USP30 are not  
453 only proximal to each other but also physically interact, either directly or indirectly. The  
454 interaction between these two proteins suggests that LETM1 may be a substrate of USP30,  
455 although this does not confirm USP30's ability to modify LETM1's ubiquitination status.

456 To further investigate, HEK293 cells were transfected with HA-Ub for 24 hours, treated with  
457 CCCP and MG132, and the ubiquitylated proteome was purified by HA pull-down in both the  
458 presence and absence of compound **39**. Upon the IP of HA-ubiquitin, LETM1 displayed  
459 increased high molecular weight laddering in the presence of compound **39**, suggesting  
460 increased LETM1 ubiquitination with USP30 inhibition (Figure 6a). This increased laddering  
461 was also phenocopied with USP30 KD (Figure 6b).

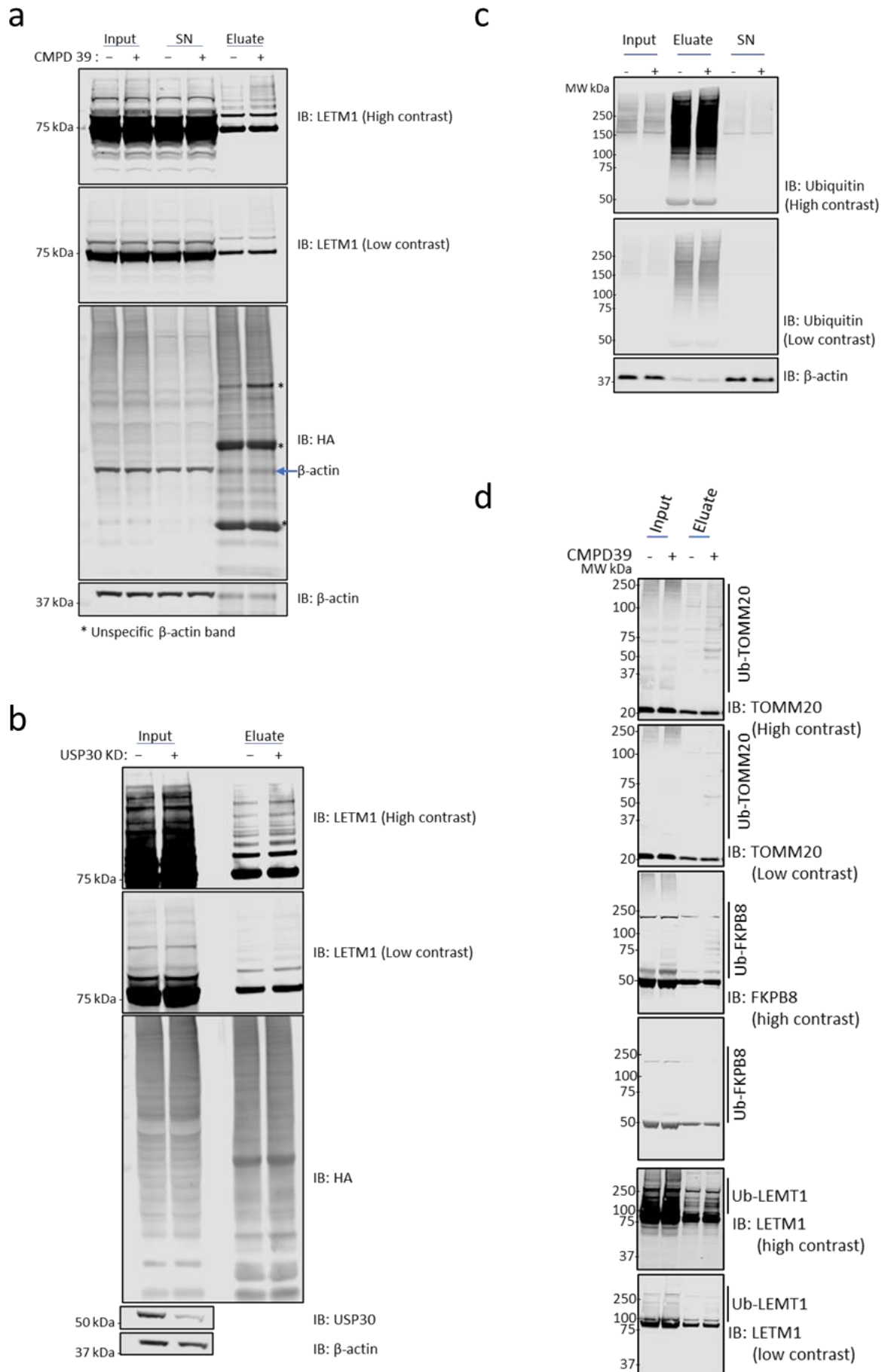
462

463 To further validate this ubiquitylation signal with an orthogonal technique, we also performed  
464 Tandem Ubiquitin Binding Entity (TUBE) pull downs on HEK293 cells treated with CCCP and  
465 +/- compound **39** (Figure 6c). Initially, we assessed the ubiquitination status of TOMM20 as  
466 a positive control, observing an accumulation of high molecular weight bands in the USP30-  
467 inhibited sample (Figure 6d). An increase in high molecular weight bands with TUBEs  
468 enrichment was also seen with FKBP8 (Figure 6d), the ubiquitination of which has previously  
469 been reported to increase with USP30 KO,<sup>22,24</sup> but has not previously been validated.

470

471 Finally, upon USP30 inhibition, LETM1 exhibited high molecular weight laddering, indicating  
472 its increased ubiquitination in the TUBE-purified ubiquitylated proteome (Figure 6d). Taken

473



474 **Figure 6 | LETM1 and FKPB8 deubiquitination are USP30 dependent. a** HA-ubiquitin pull down using anti-HA

475 antibody. HEK293T cells transiently expressing HA-Ub treated with 10  $\mu$ M CCCP +/- Compound 39. **b** HA-  
476 ubiquitin pull down using anti-HA antibody. HEK293T cells transiently transfected with scrambled or USP30  
477 siRNA and treated with 10  $\mu$ M CCCP. **(c-d)** Tandem Ubiquitin Binding Entity (TUBE) pull down in HEK293T cells  
478 treated with 10  $\mu$ M CCCP +/- Compound **39**.

479

480 together, altered LETM1 ubiquitination is arising as a direct consequence of USP30 activity,  
481 and is not due to an enzyme scaffolding function nor an off-target effect of the inhibitor.

482

## 483 **Discussion**

484

485 The study of optimizing the proximal-ubiquitome of USP30 presented here demonstrates the  
486 utility of combining the techniques of proximity labelling and ubiquitomic enrichment to  
487 elucidate direct substrates of a DUB/E3 ligase in a cellular environment. Where protein  
488 ubiquitination 'ubiquitomics' through the enrichment of the K- $\epsilon$ -GG ubiquitin remnant motif  
489 can identify global alterations in the ubiquitomic state of proteins, it does not distinguish  
490 between direct and downstream ubiquitomic events occurring upon the perturbed activity of  
491 a DUB/E3. The dynamic nature of ubiquitination events means that capturing and  
492 subsequently validating robust changes directly linked to an enzyme's activity can be  
493 challenging.

494

495 Proximity labelling is often employed to profile protein-protein interactions, including  
496 transient/weak interactions.<sup>45</sup> While proximity labelling offers a targeted insight into a  
497 protein's interactions and binding partners, here we demonstrate with APEX2 proximity  
498 labelling, that the microenvironment of USP30 is not significantly altered upon inhibition of  
499 the enzyme. In this case, it may indicate that the enrichment of those proteins proximal to  
500 USP30 alone does not inform on substrates of the enzyme itself. Additionally, high  
501 background in proximity labelling experiments means that the proteins identified in the  
502 proximitome are not exclusively interactors of a protein of interest.<sup>46</sup> The power of applying  
503 proximity labelling alone rests where large changes in protein localisation or complexes occur  
504 as a consequence of a stimulus.

505

506 Both ubiquitomic and proximity labelling studies have limitations for the identification of  
507 DUB/E3 ligase substrates when applied alone, but, when combined together, they allow for  
508 the capture of ubiquitination events proximal to the enzyme of interest. By using

509 ubiquitination as a readout, which changes when comparing an inhibited DUB/E3 ligase to a  
510 non-inhibited version, or when comparing a wild-type protein to a catalytic-dead mutant, we  
511 overcome limitations of previous methods used to identify substrates of E3 ligases, some of  
512 which cannot distinguish substrates from general protein interactors, and none of which can  
513 identify specific ubiquitination sites. Additionally, by using APEX2 to label both strong and  
514 weakly interacting substrates in the local environment around our bait protein, we overcome  
515 the limitation of IP-based methods, which typically only capture strong interactions.

516

517 Here, with USP30 as a model system, we have demonstrated that proximal-ubiquitomics  
518 enriches for events occurring in the proximity of the enzyme leading to a targeted list of  
519 positive ubiquitination hits for further validations. This was demonstrated by follow up  
520 experiments exploring LETM1 as a potentially novel USP30 substrate. LETM1 is an IMM  
521 protein, which is essential<sup>47</sup> and is key to multiple mitochondrial functions such as the  
522 maintenance of mitochondrial morphology, mitochondrial tubular network assembly and  
523 proton-dependent calcium efflux from mitochondria.<sup>30,31,48-51</sup>

524

525 Here, upon USP30 inhibition, LETM1 presented with increased ubiquitination at K292, which  
526 is proposed to be located in the mitochondrial intermembrane space.<sup>47,51</sup> We were able to  
527 detect the co-localisation of LETM1 to USP30 along with an altered ubiquitination state of  
528 LETM1 upon USP30 inhibition and knockdown. USP30 has previously been found to Co-IP with  
529 the TOMM complex,<sup>42</sup> and here we find that LETM1 also Co-IPs with TOMM20. This  
530 interaction may be upon mitochondrial import of LETM1 by the TOMM complex, or through  
531 interaction within the inter mitochondrial membrane space. Deubiquitination of proteins by  
532 USP30 may allow for them to be imported by the TOMM complex.<sup>42</sup> However, this may not  
533 be exactly clear as USP30 deubiquitination protein substrates are observed here to be  
534 predominantly located in the OMM, consistent with previous studies.<sup>22</sup> Further  
535 experimentation is needed to fully characterise these processes in greater molecular detail.

536

537 The co-localisation of USP30 to the TOMM complex was reproduced here with TOMM20-  
538 USP30 PLA and co-localisation, as well as the previously validated increase in TOMM20  
539 ubiquitination with reduced USP30 activity. We also confirmed increased ubiquitination of  
540 FKBP8 upon USP30 inhibition, which has been previously reported but not validated. The

541 TOMM complex is critical for the import of mitochondrial preproteins,<sup>52</sup> and FKBP8 has been  
542 identified as mitophagy receptor for Parkin independent mitophagy.<sup>53</sup> The presence of  
543 LETM1, TOMM20 and FKBP8 in the proximal-ubiquitome of USP30 increases the likelihood  
544 that they are direct USP30 substrates. Therefore, the proximal-ubiquitomics methodology  
545 developed here allows for an advanced insight into the action of the USP30 upon  
546 mitochondrial depolarization, and how it may be influencing the mitophagy pathway. The  
547 proximal-ubiquitomics approach builds upon previously described E3 ligase substrate  
548 detection methodologies, overcoming their limitations and allowing for the identification of  
549 specific ubiquitination events that could be applied as robust biomarkers of USP30 inhibition.  
550 More generally, proximal-ubiquitomics may be applicable more widely, not only for DUB/E3  
551 substrate discovery, but also to direct PROTAC, molecular glue and DUBTAC candidate  
552 molecule design with translational potential.

553

554

## 555 **Methods**

556

### 557 **Cell Culture**

558 Cells were incubated at 37 °C, 5 % CO<sub>2</sub>. HEK293 cells were cultured in high glucose DMEM,  
559 supplemented with 10% FBS, and 2% L-glutamine. SH-SY5Y cells were cultured in a 1:1 mix of  
560 Hams F12 nutrient Mix and EMEM, supplemented with 15 % FBS, 1 % Non-Essential amino  
561 acids and 2 mM Glutamax.

562

### 563 **Plasmid Generation**

564 The USP30-APEX2 was expressed using a pLenti-CMV-BsR-PGK-USP30-APEX-2 plasmid  
565 synthesized by Vigene Biosciences. APEX2 was conjugated to the C terminal of USP30, with a  
566 glycine/serine flexible linker. Flag-HA-USP30 was a gift from Wade Harper (Addgene plasmid  
567 # 22578 ; <http://n2t.net/addgene:22578> ; RRID:Addgene\_22578).<sup>54</sup>

568

### 569 **Lentiviral packaging**

570 HEK293T cells were plated in a T175 flask and incubated at 37 °C with 5 % CO<sub>2</sub> until they  
571 reached 85% confluency. The cells were then transfected with pMD2G, psPAX2, and the  
572 USP30-APEX2 plasmids using Lipofectamine 2000 according to the manufacturer's protocol.  
573 After two days of incubation, the supernatants were collected, filtered through a 0.45 µm  
574 filter, and subjected to ultracentrifugation to concentrate the viral particles.

575

### 576 **Cell line Generation**

577  $1.5 \times 10^5$  HEK293 cells were seeded in a 6-well plate and incubated overnight at 37 °C and 5 %  
578 CO<sub>2</sub>. 24 hrs after seeding, USP30-APEX2 lentivirus with polybrene was added to the HEK293  
579 cells at a concentration of 8 µg/ml and incubated overnight at 37 °C and 5 % CO<sub>2</sub>. 24 hrs after  
580 lentiviral treatment, the HEK293 cells were trypsinized and seeded into a 100mm dish (All  
581 cells were used). After 8 hours, 5 µg/ml blasticidin was added to both the negative control  
582 and the transduced cells. The cells were incubated for 10 days under selection, with the  
583 medium being replaced every 3 days.

584

### 585 **Transient Transfection**

586 For DNA plasmid transfections, cells were seeded in 6-well plates and transfected for 24 hrs  
587 using Lipofectamine 3000 Transfection Reagent (L3000001, ThermoFisher UK) according to  
588 the manufacturer's instructions. The concentration of plasmids used can be found in the  
589 details of each specific experiment.

590 For siRNA transfection experiments, cells were grown in 6-well plates and transfected for 72  
591 hrs with RNAiMAX Transfection Reagent (Invitrogen, 13778-150) following the  
592 manufacturer's protocol. A final concentration of 10 nM was used for the following Silencer  
593 Select siRNAs: control siRNA (4390844) and si-USP30 (Dharmacon ON-TARGETplus  
594 SMARTpool).

595

### 596 **Compound 39 synthesis**

597 'compound 39', refers to CAS number 2242582-40-5. The inhibitor was >95% pure as assessed  
598 by HPLC analysis.<sup>27</sup>

599

### 600 **HA-Ub-PA ABP labelling**

601 Ubiquitin (Gly76del) with an N-term HA tag and C-term propargylamine (HA-Ub-PA) synthesis  
602 and lysate labelling was carried out as previously described.<sup>26</sup> HEK293 expressing USP30-  
603 APEX2 were treated with compound 39 for 6 hrs at the concentration indicated in the figure,  
604 washed 3 times in PBS and lysed in 50 mM Tris (pH 7.5), 5 mM MgCl<sub>2</sub>, 0.5 mM EDTA, 250 mM  
605 sucrose and 1 mM DTT with bead beating. Lysates were then clarified at 600 xg for 10 minutes  
606 at 4 °C and supernatant protein was quantified by BCA. HA-Ub-PA was then incubated with  
607 lysate protein (1:100 w/w) for 5 minutes at 37 °C.

608

### 609 **Membrane-Cytoplasmic Cellular Fractionation**

610 As previously described<sup>39</sup>, fresh HEK293 FRT cell pellets were resuspended in digitonin lysis  
611 buffer (50 mM Hepes, pH 7.5, 10 mg/ml digitonin, 150 mM NaCl) and incubated for 30  
612 minutes at 4°C with continuous agitation. The sample was then centrifuged at 6,000g for 5  
613 minutes at 4°C. The resulting supernatant, containing the cytoplasmic fraction, was carefully  
614 transferred to a new tube. The pellet was resuspended in a buffer containing 0.3% NP-40, 50  
615 mM Hepes (pH 7.5), and 150 mM NaCl, and incubated on ice for 5 minutes. After  
616 centrifugation at 1,500g for 5 minutes, the supernatant, representing the membrane fraction,  
617 was collected into a separate tube and stored at -20°C until further analysis.

618

### 619 **Proximal ubiquitomics workflow - APEX2 proximity labelling**

620 HEK293 cells expressing USP30-APEX2 were grown in T175 flasks coated with Poly-D-Lysine  
621 to 100 % confluency, with 5 x T175 flasks pooled per condition. The medium was then  
622 replaced with fresh medium containing 10  $\mu$ M CCCP, with either 5  $\mu$ M of compound **39**, or  
623 DMSO as a control. The cells were incubated at 37°C and 5% CO<sub>2</sub> for 5.5 hours. Following this  
624 incubation, proximity labelling was performed as previously described.<sup>34,46,55</sup> Briefly, 2  $\mu$ M  
625 phenol biotin was added to the media, and the cells were incubated for an additional 30  
626 minutes. Subsequently, H<sub>2</sub>O<sub>2</sub> at a concentration of 1 mM was added to the medium for exactly  
627 1 minute. The cells were then washed four times with Quencher buffer (10 mM sodium  
628 ascorbate, 10 mM sodium azide, 5mM Trolox in DPBS), with each wash involving a 1-minute  
629 incubation.

630 The cells were lysed using lysis buffer (10 ml per 5 x T175 flasks) (RIPA lysis buffer containing  
631 1 mM PMSF, 5 mM Trolox, 10 mM sodium azide, 10 mM sodium ascorbate, PhosSTOP  
632 phosphatase inhibitor and cOmplete Protease Inhibitor Cocktail) and centrifuged at 10,000  
633 *xg* for 10 minutes at 4°C. At this stage 5% of lysate was taken for the 'labelled proteome' and  
634 processed for mass spectrometry analysis using the S-Trap™ micro digestion protocol  
635 according to the manufacturer's instructions. and the remain lysate was incubated with 3.5  
636 mL of streptavidin agarose beads for 1 hour at room temperature. The beads were then  
637 washed with 10 mL of the following buffers in the specified order: twice with RIPA buffer,  
638 then with KCl, Na<sub>2</sub>CO<sub>3</sub>, 2M Urea, 1% SDS and finally with 2 times with RIPA buffer.

639 Biotinylated proteins were eluted in 4 mL of 2x loading dye supplemented with 2 mM biotin  
640 and 20 mM DTT by boiling (98°C) for 10 min. Eluted material was subsequently processed for  
641 mass spectrometry analysis using the S-Trap™ midi digestion protocol according to the  
642 manufacturer's instructions. 10 % of eluates from the S-Trap™ clean up were taken for LC-  
643 MS/MS analysis as the 'proximitome'.

644

### 645 **Proximal ubiquitomics workflow - K- $\epsilon$ -GG immunoprecipitation**

646 The subsequent K- $\epsilon$ -GG immunoprecipitation (IP) was performed according to the  
647 manufacturer's instructions with small differences. Briefly, lyophilized peptides were  
648 centrifuged for 5 minutes at 2000 *xg* at room temperature. To the dried peptides, 0.5 mL of  
649 1X IAP bind buffer was added, and the peptides were resuspended mechanically by repeated

650 pipetting. The solution was then centrifuged for 5 minutes at 10,000  $xg$  at 4°C and transferred  
651 into a new Eppendorf tube.

652 For each sample, 10  $\mu$ L of bead slurry was placed into a 1.5 mL Eppendorf tube. The beads  
653 were washed four times with 1 mL of ice-cold PBS. The soluble peptides were then transferred  
654 to the beads and incubated on an end-over-end rotator for 2 hours at 4°C. Afterwards, the  
655 samples were spun down at 2000  $xg$  for 5 seconds to pellet the beads, placed on a magnetic  
656 rack for 10 seconds, and the unbound peptide solution was discarded.

657 The beads were washed with 1 mL of chilled HS IAP Wash Buffer (1X), resuspended, briefly  
658 centrifuged as before, placed on the magnetic rack for 10 seconds, and the wash buffer was  
659 removed. This washing step was repeated three additional times. The samples were then  
660 washed twice with 1 mL of chilled LCMS water. Ubiquitinated peptides were eluted by adding  
661 50  $\mu$ L of IAP Elution buffer and incubating at room temperature for 10 minutes with gentle  
662 mixing. The elution was repeated once more to ensure complete recovery of ubiquitinated  
663 peptides. Peptides were then purified by C18 and resuspended in 5% DMSO/5% FA for LC-  
664 MS/MS analysis.

665 The input material optimization shown in Figure 2g-h follow this USP30-APEX2 proximity  
666 labelling workflow with indicated number of 15 cm dishes as input.

667

#### 668 **Control proteome, control ubiquitome and labelled ubiquitome**

669 HEK293 cells expressing USP30-APEX2 were grown in 10 cm dishes coated with Poly-D-Lysine  
670 to 100 % confluency, with 1 x 10 cm dish used per condition. Cells were APEX2 labelled as  
671 detailed for the proximal-ubiquitome for the 'labelled ubiquitome'. Cells for the control  
672 proteome and control ubiquitome were not APEX2 labelled. Cells were treated with CCCP +/-  
673 compound **39**, lysed in 500  $\mu$ L, clarified and processed using S-Trap™ midi as detailed for the  
674 proximal-ubiquitome. Where cells were not APEX2 labelled, 5% was removed for the control  
675 proteome. Remaining peptides were then K- $\epsilon$ -GG immunoprecipitated as detailed for the  
676 proximal-ubiquitome.

677

#### 678 **Liquid chromatography tandem mass spectrometry - LC-MS/MS**

679 The proximal-ubiquitome was analysed on a timsTOF SCP (Bruker) LC-MS/MS system to  
680 maximise sensitivity. The input material optimization detailed in Figure 2g-h was analysed on

681 an Orbitrap Fusion Lumos Tribid (Thermo) LC-MS/MS system. All other samples were analysed  
682 on an Orbitrap Ascend Tribid (Thermo) LC-MS/MS system.

683

684 APEX2 proximitome and total proteomics samples were analysed by LC-MS/MS using a  
685 Vanquish Neo UHPLC (Thermo) connected to a Thermo Orbitrap Ascend mass spectrometer  
686 (Thermo). The Vanquish Neo was operated in “Trap and Elute” mode using a PepMap Neo  
687 trap (185um, 300um x 5mm) and EASY-SPRAY PepMapNeo column (50cmx75um, 1500bar).  
688 Tryptic peptides were trap and separated using a 60 min linear gradient over 60 minutes (from  
689 3 to 20% B in 40 min and from 20 to 35% in 20 min) at 300nl/min flow.

690 APEX proximitome and total proteomics samples were acquired in DIA mode with some slight  
691 changes from previously described method.<sup>27,56</sup> Briefly, survey scans (MS1) were acquired in  
692 the Orbitrap over the mass range of 350 – 1650m/z, with a 45k resolution, maximum injection  
693 time of 91 ms, an AGC set to 125% and a RF lens at 30%. MS2 scans were then collected using  
694 the tMSn scan function, with a 40 predefined variable width DIA scan windows<sup>56</sup> with a 30K  
695 orbitrap resolution, normalized AGC target of 1000%, maximum injection time set to auto and  
696 a 30 % collision energy.

697 K-ε-GG enriched ubiquitomics samples were analysed by LC-MS/MS using an Ultimate 3000  
698 HPLC coupled to an Orbitrap Ascend Tribid or an Orbitrap Fusion Lumos Tribid instrument  
699 (Thermo Fisher) using a nano-EASY spray source. Tryptic peptides were loaded onto an  
700 AcclaimPepMap100 trap column (100µm x 2cm, PN164750; ThermoFisher) and separated on  
701 a 50cm EasySpray column (ES903, ThermoFisher) using a 60 min linear gradient from 2 to 35%  
702 acetonitrile, 0.1% formic acid and at 250nl/min flow rate. Both trap and column were kept at  
703 50C. Data were acquired in DIA-mode with 44 variable width windows optimised for GG  
704 workflows as previously described.<sup>37</sup> In brief, MS1 scans were acquired in the Orbitrap over  
705 the mass range of 350 – 1650m/z, with a 120k resolution, maximum injection time of 60ms,  
706 an AGC set to 300% and a RF lens at 30%. MS2 scans were then collected using the tMSn scan  
707 function, with a 44 predefined variable width DIA scan windows<sup>37</sup> with a 30K orbitrap  
708 resolution, normalized AGC target of 2000%, maximum injection time set to auto and HCD  
709 stepped collision energy set at 22, 27 and 30 %.

710

711 Proximal-ubiquitome samples were analysed using an EvoSep One LC system (EvoSep)  
712 coupled to a timsTOF SCP mass spectrometer (Bruker) using the Whisper 40 samples per day

713 method and a 75  $\mu\text{m}$  x 150 mm C18 column with 1.7  $\mu\text{m}$  particles and an integrated Captive  
714 Spray Emitter (IonOpticks). Buffer A was 0.1% formic acid in water, Buffer B was 0.1% formic  
715 acid in acetonitrile. Data was collected using diaPASEF<sup>57</sup> with 1 MS frame and 9 diaPASEF  
716 frames per cycle with an accumulation and ramp time of 100 ms, for a total cycle time of  
717 1.07 seconds. The diaPASEF frames were separated into 3 ion mobility windows, in total  
718 covering the 400 – 1000 m/z mass range with 25 m/z-wide windows between an ion mobility  
719 range of 0.64–1.4 Vs/cm<sup>2</sup>. The collision energy was ramped linearly over the ion mobility  
720 range, with 20 eV applied at 0.6 Vs/cm<sup>2</sup> to 59 eV at 1.6 Vs/cm<sup>2</sup>.

721

### 722 **LC-MS/MS data processing**

723

724 All data were searched library-free with DIA-NN 1.8.1<sup>37,58</sup> with a Uniprot *Homo Sapiens* fasta  
725 (20,370 entries, retrieved on April 16, 2021). For ubiquitome searches all settings were left as  
726 default other than the addition of variable modifications (methionine oxidation, N-terminal  
727 acetylation and K- $\epsilon$ -GG ubiquitin remnant motif, with a maximum of 2 variable modifications  
728 allowed). Default search settings include 1 missed Trypsin/P cleavage, with fixed N-terminal  
729 methionine excision and fixed cysteine carbamidomethylation. For proteome and  
730 proximitome searches, settings were identical other than the K- $\epsilon$ -GG variable modification.  
731 Match-between runs was enabled for all searches, except for the input material optimization  
732 in Figure 2g-h.

733

### 734 **LC-MS/MS data analysis**

735 For ubiquitome data, peptide level information was extracted from the DIA-NN precursor  
736 matrix output. The output was filtered to remove any non-proteotypic identifications,  
737 collapsed to provide peptide level information by summing precursors with different charge  
738 states using R (version 4.3.2), and filtered for the UniMod:121 K- $\epsilon$ -GG adduct. For  
739 proximitome and proteome data, the DIA-NN protein groups output matrix was used. All data  
740 was imported into Perseus (Version 1.6.15.0),<sup>59</sup> log<sub>2</sub> transformed, filtered so that values were  
741 present in all replicates for at least 1 condition, median subtract normalised, and imputed  
742 using imputeLCMD k-nearest neighbour (KNN) with a neighbour number of 15. A Perseus two-  
743 sample students T-test with permutation-based FDR set to 5 % was applied to extract  
744 significant changes as indicated in figures.

745

#### 746 **Permutation analysis of proximitome vs proteome**

747 Permutation analysis was carried out in R to establish the significance of the increased  
748 intensity of OMM proteins in the proximitome vs the proteome, when compared to all  
749 proteins and to those in the MM. This was achieved by multiplying the difference of each  
750 protein between the proximitome vs the proteome randomly by either +1 or -1 100000 times  
751 and then plotting the means of the differences as a distribution and comparing this to the  
752 mean difference of Mitocarta 3.0 annotated OMM proteins, MM proteins and to the proteins  
753 overall.

754

#### 755 **Immunofluorescence/Proximity ligation assay**

756 Cells were fixed with 4% paraformaldehyde at room temperature for 10 minutes, followed by  
757 three washes with PBS. Next, the cells were incubated with PBS containing 0.1% Triton-X-100  
758 for 10 minutes at room temperature, followed by a PBS wash for 5 minutes. Subsequently,  
759 the cells were blocked with 5% BSA in TBST containing 0.1% Tween 20 for 1 hour.

760 Depending on the sample, the cells were then incubated with the following primary  
761 antibodies: ANTI-FLAG® M1 (1:1000) (Sigma Aldrich F3040), LETM1 (1:100) (Proteintech,  
762 16024-1-AP), and TOMM20 (1:100) (Cell Signaling, 42406) at 4 °C overnight. After primary  
763 antibody incubation, the cells were washed three times with TBST containing 0.1% Tween 20,  
764 incubating with the wash buffer for 5 minutes each time.

765 For the proximity ligation assay (PLA), the cells were incubated with PLA anti-mouse PLUS and  
766 anti-rabbit MINUS Duolink secondaries, followed by Duolink In Situ Orange Reagents,  
767 according to the manufacturer's protocol (Millipore Sigma).

768 For immunofluorescence, the cells were incubated with the secondary antibodies (Goat anti-  
769 Mouse IgG (H + L), Alexa Fluor 488-conjugated, and Goat anti-Rabbit IgG (H + L), Alexa Fluor  
770 633-conjugated) in 1% BSA in TBST containing 0.1% Tween 20 for 1 hour at room temperature.

771 The cells were then washed three times with TBST containing 0.1% Tween 20, incubating with  
772 the wash buffer for 5 minutes each time.

773 For nuclear staining, the cells were incubated with Hoechst 33342 (1:1000) for 10 minutes at  
774 room temperature, followed by three washes with PBS.

775 Samples from both PLA and immunofluorescence were imaged using a high-content laser-  
776 based spinning disk confocal microscope (Opera Phenix Plus) with a 40x water objective.  
777 Images were collected and analyzed using Harmony® imaging and analysis software.  
778 For colocalisation analysis, the images were processed using ImageJ, and Li's Intensity  
779 Correlation Quotient (ICQ) was calculated using the Coloc 2 plugin.

780

## 781 **Immunoprecipitation**

782 **IP-Flag:** Cells were washed twice with ice-cold PBS and then lysed in Pierce IP lysis buffer (25  
783 mM Tris-HCl pH 7.4, 150 mM NaCl, 1% NP-40, 1 mM EDTA, 5% glycerol, PhosSTOP  
784 phosphatase inhibitor, and cOmplete Protease Inhibitor Cocktail). The lysates were incubated  
785 on ice for 10 minutes with periodic mixing and then clarified by centrifugation at 13,000  $xg$   
786 for 10 minutes at 4°C. The pre-cleared lysates were incubated with anti-FLAG M2 Magnetic  
787 Beads at 4°C for 4 hours. After washing three times with lysis buffer, the proteins bound to  
788 the anti-FLAG antibody were pulled down by 3X FLAG peptide elution buffer. Both the whole  
789 cell lysates and the pull-down samples were subjected to immunoblotting analysis.

790 **IP-LETM1:** Cells were washed twice with ice-cold PBS and then lysed in Pierce IP lysis buffer  
791 (25 mM Tris-HCl pH 7.4, 150 mM NaCl, 1% NP-40, 1 mM EDTA, 5% glycerol, PhosSTOP  
792 phosphatase inhibitor, and cOmplete Protease Inhibitor Cocktail). The lysates were incubated  
793 on ice for 10 minutes with periodic mixing and then clarified by centrifugation at 13,000 g for  
794 10 minutes at 4°C to remove cell debris. The pre-cleared lysates were incubated with anti-  
795 LETM1 antibody in a dilution of 1:100. The next day, lysates were incubated with 50 $\mu$ L of  
796 Dynabeads™ Protein G for Immunoprecipitation and incubated for 30 minutes at room  
797 temperature. After washing three times with lysis buffer, the proteins bound to the anti-  
798 LETM1 antibody were eluted by 2X Loading dye and 100mM DTT elution buffer. Both the  
799 whole cell lysates and the pull-down samples were subjected to immunoblotting analysis.

800

## 801 **Tandem ubiquitin binding entity pulldown**

802 HEK293 cells were grown in 150 mm dish to 100% confluency, with 1 x 150 mm dish per  
803 condition. The medium was then replaced with fresh medium containing 10  $\mu$ M CCCP, with  
804 either 5  $\mu$ M of compound **39**, or DMSO as a control. The cells were incubated at 37 °C and 5  
805 % CO<sub>2</sub> for 6 hours. Cells were washed twice with ice-cold PBS and then lysed in Pierce IP lysis  
806 buffer (25 mM Tris-HCl pH 7.4, 150 mM NaCl, 1% NP-40, 1 mM EDTA, 5% glycerol, PhosSTOP

807 phosphatase inhibitor, and cOmplete Protease Inhibitor Cocktail, 100mM N-Ethylmaleimide  
808 (NEM) and 10  $\mu$ M MG132). The lysates were incubated on ice for 10 minutes with periodic  
809 mixing and then clarified by centrifugation at 13,000 g for 10 minutes at 4°C to remove cell  
810 debris. Supernatant was collected and 10 % of sample was removed as "INPUT" for analysis  
811 by Western blotting. Endogenous ubiquitylated proteins were isolated from the soluble lysate  
812 at 4 °C for 12 hrs using 50  $\mu$ l of packed agarose TUBE (TUBE1, Life sensors, performed  
813 according to the manufacturer's instructions). Following four washes in TBST, bound proteins  
814 were eluted using reducing and denaturing SDS sample loading buffer and analysed by  
815 Western blot.

816

### 817 **Data availability**

818 The mass spectrometry proteomics data have been deposited to the ProteomeXchange  
819 Consortium via the PRIDE<sup>60</sup> partner repository with the dataset identifier PXD054890.

820

821

822

823

824

825

826

827

828

## 829 References

- 830 1. Zuin, A., Isasa, M. & Crosas, B. Ubiquitin Signaling: Extreme Conservation as a Source  
831 of Diversity. *Cells* **3**, 690–701 (2014).
- 832 2. Wilkinson, K. D. Ubiquitin-Dependent Signaling: The Role of Ubiquitination in the  
833 Response of Cells to Their Environment. *J Nutr* **129**, 1933–1936 (1999).
- 834 3. Reyes-Turcu, F. E., Ventii, K. H. & Wilkinson, K. D. Regulation and Cellular Roles of  
835 Ubiquitin-Specific Deubiquitinating Enzymes. *Annu Rev Biochem* **78**, 363–397 (2009).
- 836 4. Deng, L., Meng, T., Chen, L., Wei, W. & Wang, P. The role of ubiquitination in  
837 tumorigenesis and targeted drug discovery. *Signal Transduct Target Ther* **5**, 11 (2020).
- 838 5. Le Guerroué, F. & Youle, R. J. Ubiquitin signaling in neurodegenerative diseases: an  
839 autophagy and proteasome perspective. *Cell Death Differ* **28**, 439–454 (2021).
- 840 6. Harrigan, J. A., Jacq, X., Martin, N. M. & Jackson, S. P. Deubiquitylating enzymes and  
841 drug discovery: emerging opportunities. *Nat Rev Drug Discov* **17**, 57–78 (2018).
- 842 7. O'Connor, H. F. *et al.* Ubiquitin-Activated Interaction Traps (UBAITs) identify E3 ligase  
843 binding partners. *EMBO Rep* **16**, 1699–1712 (2015).
- 844 8. Kumar, R., González-Prieto, R., Xiao, Z., Verlaan-de Vries, M. & Vertegaal, A. C. O. The  
845 STUbl RNF4 regulates protein group SUMOylation by targeting the SUMO  
846 conjugation machinery. *Nat Commun* **8**, 1809 (2017).
- 847 9. Salas-Lloret, D., Agabiti, G. & González-Prieto, R. TULIP2: An Improved Method for  
848 the Identification of Ubiquitin E3-Specific Targets. *Front Chem* **7**, 802 (2019).
- 849 10. Bhuripanyo, K. *et al.* Identifying the substrate proteins of U-box E3s E4B and CHIP by  
850 orthogonal ubiquitin transfer. *Sci Adv* **4**, (2018).
- 851 11. Wang, Y. *et al.* Identifying the ubiquitination targets of E6AP by orthogonal ubiquitin  
852 transfer. *Nat Commun* **8**, 2232 (2017).
- 853 12. Mukhopadhyay, U. *et al.* A ubiquitin-specific, proximity-based labeling approach for  
854 the identification of ubiquitin ligase substrates. *Sci Adv* **10**, (2024).
- 855 13. Barroso-Gomila, O. *et al.* BioE3 identifies specific substrates of ubiquitin E3 ligases.  
856 *Nat Commun* **14**, 7656 (2023).
- 857 14. Bustos, D., Bakalarski, C. E., Yang, Y., Peng, J. & Kirkpatrick, D. S. Characterizing  
858 Ubiquitination Sites by Peptide-based Immunoaffinity Enrichment. *Molecular &*  
859 *Cellular Proteomics* **11**, 1529–1540 (2012).
- 860 15. Peng, J. *et al.* A proteomics approach to understanding protein ubiquitination. *Nat*  
861 *Biotechnol* **21**, 921–926 (2003).
- 862 16. Roux, K. J., Kim, D. I., Raida, M. & Burke, B. A promiscuous biotin ligase fusion protein  
863 identifies proximal and interacting proteins in mammalian cells. *Journal of Cell*  
864 *Biology* **196**, 801–810 (2012).
- 865 17. Lam, S. S. *et al.* Directed evolution of APEX2 for electron microscopy and proximity  
866 labeling. *Nat Methods* **12**, 51–54 (2015).
- 867 18. Huang, Y. *et al.* A proximity labeling-based orthogonal trap strategy identifies HDAC8  
868 promotes cell motility by modulating cortactin acetylation. *Cell Chem Biol* **31**, 514-  
869 522.e4 (2024).
- 870 19. Liu, Y. *et al.* Spatiotemporally resolved subcellular phosphoproteomics. *Proceedings*  
871 *of the National Academy of Sciences* **118**, (2021).
- 872 20. Geoghegan, V. *et al.* CLK1/CLK2-driven signalling at the Leishmania kinetochore is  
873 captured by spatially referenced proximity phosphoproteomics. *Commun Biol* **5**, 1305  
874 (2022).

- 875 21. Fang, T.-S. Z. *et al.* Knockout or inhibition of USP30 protects dopaminergic neurons in  
876 a Parkinson's disease mouse model. *Nat Commun* **14**, 7295 (2023).
- 877 22. Rusilowicz-Jones, E. V. *et al.* USP30 sets a trigger threshold for PINK1–PARKIN  
878 amplification of mitochondrial ubiquitylation. *Life Sci Alliance* **3**, (2020).
- 879 23. Nakamura, N. & Hirose, S. Regulation of Mitochondrial Morphology by USP30, a  
880 Deubiquitinating Enzyme Present in the Mitochondrial Outer Membrane. *Mol Biol*  
881 *Cell* **19**, 1903–1911 (2008).
- 882 24. Ordureau, A. *et al.* Global Landscape and Dynamics of Parkin and USP30-Dependent  
883 Ubiquitylomes in iNeurons during Mitophagic Signaling. *Mol Cell* **77**, 1124–1142.e10  
884 (2020).
- 885 25. Rusilowicz-Jones, E. V *et al.* Benchmarking a highly selective USP30 inhibitor for  
886 enhancement of mitophagy and pexophagy. *Life Sci Alliance* **5**, e202101287 (2022).
- 887 26. Jones, H. B. L., Heilig, R., Fischer, R., Kessler, B. M. & Pinto-Fernández, A. ABPP-HT -  
888 High-Throughput Activity-Based Profiling of Deubiquitylating Enzyme Inhibitors in a  
889 Cellular Context. *Front Chem* **9**, 44 (2021).
- 890 27. O'Brien, D. P. *et al.* Structural Premise of Selective Deubiquitinase USP30 Inhibition by  
891 Small-Molecule Benzosulfonamides. *Mol Cell Proteomics* **22**, 100609 (2023).
- 892 28. Shao, J. *et al.* Leucine zipper-EF-hand containing transmembrane protein 1 (LETM1)  
893 forms a Ca<sup>2+</sup>/H<sup>+</sup> antiporter. *Sci Rep* **6**, 34174 (2016).
- 894 29. Piao, L. *et al.* Regulation of OPA1-mediated mitochondrial fusion by leucine zipper/EF-  
895 hand-containing transmembrane protein-1 plays a role in apoptosis. *Cell Signal* **21**,  
896 767–777 (2009).
- 897 30. Dimmer, K. S. *et al.* LETM1, deleted in Wolf Hirschhorn syndrome is required for  
898 normal mitochondrial morphology and cellular viability. *Hum Mol Genet* **17**, 201–214  
899 (2007).
- 900 31. Tamai, S. *et al.* Characterization of the mitochondrial protein LETM1, which maintains  
901 the mitochondrial tubular shapes and interacts with the AAA-ATPase BCS1L. *J Cell Sci*  
902 **121**, 2588–2600 (2008).
- 903 32. Qin, J. Y. *et al.* Systematic Comparison of Constitutive Promoters and the Doxycycline-  
904 Inducible Promoter. *PLoS One* **5**, e10611 (2010).
- 905 33. Pinto-Fernández, A. *et al.* Comprehensive Landscape of Active Deubiquitinating  
906 Enzymes Profiled by Advanced Chemoproteomics. *Front Chem* **7**, 592 (2019).
- 907 34. Liang, Z. *et al.* Protocol to profile spatially resolved NLRP3 inflammasome complexes  
908 using APEX2-based proximity labelling. *STAR Protoc* **In review**,.
- 909 35. Kim, W. *et al.* Systematic and quantitative assessment of the ubiquitin-modified  
910 proteome. *Mol Cell* **44**, 325–340 (2011).
- 911 36. Vere, G., Kealy, R., Kessler, B. M. & Pinto-Fernandez, A. Ubiquitomics: An overview  
912 and future. *Biomolecules* vol. 10 1–22 Preprint at  
913 <https://doi.org/10.3390/biom10101453> (2020).
- 914 37. Steger, M. *et al.* Time-resolved in vivo ubiquitinome profiling by DIA-MS reveals USP7  
915 targets on a proteome-wide scale. *Nat Commun* **12**, 5399 (2021).
- 916 38. Wang, M., Herrmann, C. J., Simonovic, M., Szklarczyk, D. & von Mering, C. Version 4.0  
917 of PaxDb: Protein abundance data, integrated across model organisms, tissues, and  
918 cell-lines. *Proteomics* **15**, 3163–3168 (2015).
- 919 39. Geiger, T., Wehner, A., Schaab, C., Cox, J. & Mann, M. Comparative Proteomic  
920 Analysis of Eleven Common Cell Lines Reveals Ubiquitous but Varying Expression of  
921 Most Proteins. *Molecular & Cellular Proteomics* **11**, M111.014050 (2012).

- 922 40. Szklarczyk, D. *et al.* The STRING database in 2023: protein–protein association  
923 networks and functional enrichment analyses for any sequenced genome of interest.  
924 *Nucleic Acids Res* **51**, D638–D646 (2023).
- 925 41. Imlay, J. A., Chin, S. M. & Linn, S. Toxic DNA Damage by Hydrogen Peroxide Through  
926 the Fenton Reaction in Vivo and in Vitro. *Science (1979)* **240**, 640–642 (1988).
- 927 42. Phu, L. *et al.* Dynamic Regulation of Mitochondrial Import by the Ubiquitin System.  
928 *Mol Cell* **77**, 1107–1123.e10 (2020).
- 929 43. Fang, T.-S. Z. *et al.* Knockout or inhibition of USP30 protects dopaminergic neurons in  
930 a Parkinson’s disease mouse model. *Nat Commun* **14**, 7295 (2023).
- 931 44. Shannon, P. *et al.* Cytoscape: A Software Environment for Integrated Models of  
932 Biomolecular Interaction Networks. *Genome Res* **13**, 2498–2504 (2003).
- 933 45. Bosch, J. A., Chen, C. & Perrimon, N. Proximity-dependent labeling methods for  
934 proteomic profiling in living cells: An update. *WIREs Developmental Biology* **10**, e392  
935 (2021).
- 936 46. Damianou, A. *et al.* Oncogenic mutations of KRAS modulate its turnover by the  
937 CUL3/LZTR1 E3 ligase complex. *Life Sci Alliance* **7**, e202302245 (2024).
- 938 47. Austin, S. & Nowikovsky, K. LETM1: Essential for Mitochondrial Biology and Cation  
939 Homeostasis? *Trends Biochem Sci* **44**, 648–658 (2019).
- 940 48. Tamai, S. *et al.* Characterization of the mitochondrial protein LETM1, which maintains  
941 the mitochondrial tubular shapes and interacts with the AAA-ATPase BCS1L. *J Cell Sci*  
942 **121**, 2588–2600 (2008).
- 943 49. Jiang, D., Zhao, L. & Clapham, D. E. Genome-Wide RNAi Screen Identifies Letm1 as a  
944 Mitochondrial Ca<sup>2+</sup>/H<sup>+</sup> Antiporter. *Science (1979)* **326**, 144–147 (2009).
- 945 50. Tsai, M.-F., Jiang, D., Zhao, L., Clapham, D. & Miller, C. Functional reconstitution of  
946 the mitochondrial Ca<sup>2+</sup>/H<sup>+</sup> antiporter Letm1. *Journal of General Physiology* **143**, 67–  
947 73 (2014).
- 948 51. Natarajan, G. K., Mishra, J., Camara, A. K. S. & Kwok, W. M. LETM1: A Single Entity  
949 With Diverse Impact on Mitochondrial Metabolism and Cellular Signaling. *Front*  
950 *Physiol* **12**, 637852 (2021).
- 951 52. Araiso, Y. *et al.* Structure of the mitochondrial import gate reveals distinct preprotein  
952 paths. *Nature* **575**, 395–401 (2019).
- 953 53. Bhujabal, Z. *et al.* FKBP8 recruits LC3A to mediate Parkin-independent mitophagy.  
954 *EMBO Rep* **18**, 947–961 (2017).
- 955 54. Sowa, M. E., Bennett, E. J., Gygi, S. P. & Harper, J. W. Defining the Human  
956 Deubiquitinating Enzyme Interaction Landscape. *Cell* **138**, 389–403 (2009).
- 957 55. Liang, Z. *et al.* Proximity proteomics reveals UCH-L1 as an essential regulator of  
958 NLRP3-mediated IL-1 $\beta$  production in human macrophages and microglia. *Cell Rep* **43**,  
959 114152 (2024).
- 960 56. Muntel, J. *et al.* Comparison of Protein Quantification in a Complex Background by  
961 DIA and TMT Workflows with Fixed Instrument Time. *J Proteome Res* **18**, 1340–1351  
962 (2019).
- 963 57. Meier, F. *et al.* diaPASEF: parallel accumulation–serial fragmentation combined with  
964 data-independent acquisition. *Nature Methods* **2020 17:12** **17**, 1229–1236 (2020).
- 965 58. Demichev, V., Messner, C. B., Vernardis, S. I., Lilley, K. S. & Ralser, M. DIA-NN: neural  
966 networks and interference correction enable deep proteome coverage in high  
967 throughput. *Nat Methods* **17**, 41–44 (2020).

- 968 59. Tyanova, S. *et al.* The Perseus computational platform for comprehensive analysis of  
969 (prote)omics data. *Nat Methods* **13**, 731–740 (2016).  
970 60. Perez-Riverol, Y. *et al.* The PRIDE database resources in 2022: a hub for mass  
971 spectrometry-based proteomics evidences. *Nucleic Acids Res* **50**, D543–D552 (2022).  
972

## 973 **Acknowledgements**

974 We thank members of the Kessler and ODDI groups for helpful discussions. We also thank Val  
975 Miller and Daniel Ebner for using and guiding us with confocal microscopy. We would like to  
976 express our gratitude to Jesper Hansen for his guidance in analyzing the colocalization  
977 experiments. We thank Daryl S. Walter from Evotec for providing us with an aliquot of  
978 compound 39. H.B.L.J. was supported by a Bristol-Myers Squibb fellowship. A.D., S.D., and  
979 B.M.K. were supported by the Chinese Academy of Medical Sciences (CAMS) Innovation Fund  
980 for Medical Science (CIFMS), China [grant number: 2018-I2M-2-002], and B.M.K. by the  
981 Engineering and Physical Sciences Research Council (EPSRC) grant [number: EP/N034295/1].  
982

## 983 **Author contributions**

984 A.D and H.B.L.J contributed equally. A.D., H.B.L.J and B.M.K conceptualized the study. A.D,  
985 H.B.L.J, A.G., I.V. and S.D. conducted experiments. H.B.L.J and A.D. analysed data. B.M.K.  
986 supervised the experimental work. Funding was acquired by B.M.K. All authors wrote and  
987 approved the paper.

988

## 989 **Ethics declaration**

### 990 **Competing interests**

991 The authors declare that they have no competing interests affecting the contents of this  
992 article.

993

## 994 **Corresponding authors**

995 Correspondence to H.B.L.J, A.D. or B.M.K.

996

997

998